An area-based approach for estimating extreme precipitation probability

Peng Gao[1,*], Gregory J. Carbone[1], Junyu Lu[1] and Diansheng Guo[1]

[1] Department of Geography, University of South Carolina, 709 Bull Street, Columbia, SC 29208, USA

[*] Department of Geography, University of South Carolina, 709 Bull Street, Columbia, SC 29208, USA. Tel.: +1 803 777 6746. Email: gaop@mailbox.sc.edu. Corresponding Author.

Abstract

Accurate estimates of heavy rainfall probabilities reduce loss of life, property, and infrastructure failure resulting from flooding. NOAA's *Atlas-14* provides point-based precipitation exceedance probability estimates for a range of durations and recurrence intervals. While it has been used as an engineering reference, *Atlas-14* does not provide direct estimates of *areal* rainfall totals which provide a better predictor of flooding that leads to infrastructure failure, and more relevant input for storm water or hydrologic modeling. This study produces heavy precipitation exceedance probability estimates based on basin-level precipitation totals. We adapted a Generalized Extreme Value (GEV) distribution to estimate Intensity-Duration-Frequency (IDF) curves from annual maximum totals. The method exploits a high-resolution precipitation data set and uses a bootstrapping approach to borrow spatially across homogeneous regions, substituting space in lieu of long time series. We compared area-based estimates of 1-, 2-, and 4-day annual maximum total probabilities against point-based estimates at rain gauges within watersheds impacted by five recent extraordinary precipitation and flooding events. We found considerable differences between point-based and area-based estimates. It suggests that caveats are needed when using pointed-based estimates to represent areal estimates as model inputs for the purpose of storm water management and flood risk assessment.

Key words: precipitation extremes, Intensity-Duration-Frequency (IDF) curves, NOAA *Atlas - 14*

Introduction

Extreme rainfall and consequent flooding cause tremendous loss of life and property, and infrastructure failure (Merz et al. 2010). During the past 30 years, floods have claimed a national average of 82 lives and caused approximately $8B in damages annually (National Weather Service, 2016). Individual events have caused losses in concentrated areas, such as the heavy rainfall and October 2015 flooding in South Carolina that resulted in $130m paid losses and the failure of 52 dams (FEMA, 2017; SCDHEC, 2017). A Louisiana flood in May 1995 led to $585m paid losses (FEMA, 2017). Understanding the probability of heavy rainfall events aids the design and operation of infrastructure that could mitigate losses from such hydrologic hazards (Zhu 2013).

Extreme rainfall is typically summarized with Intensity-Duration-Frequency (IDF) curves that describe the relationship between rainfall intensity, rainfall duration and return period (or its reverse, probability of exceedance). IDF curves are typically derived from rainfall measurements or model outputs. For every year of record, annual maximum rainfall intensity for specific durations (e.g., 1 hour, 1 day, 2 days) is determined. A variety of distributions (e.g., Generalized Extreme Value distribution, Pearson Type III distribution, and Generalized Pareto distribution) and statistical methods (e.g., L-moments and maximum-likelihood) could be used to estimate probabilities of exceedance and fit curves (Guttman 1993; Mailhot et al. 2007; Peck, Prodanovic, and Simonovic 2012; Willems et al. 2012; Zhu et al. 2013; Mirhosseini, Srivastava, and Stefanova 2013; Soltani et al. 2017). From these, one derives synthetic design storms which are then used to appropriately size infrastructure, such as dams and urban drainage systems. For instance, in Norway, the probable maximum precipitation is applied along with the 500- or 1000-year return levels for dam design and flood preparation (Dyrrdal et al. 2016). Estimation of IDF

is usually derived from long records observed at rain gauges. For example, in the United States, NOAA's *Atlas-14* which provides point-based precipitation probability exceedance estimates for a range of durations (5- minute to 60-day) and recurrence intervals (1-1000 years) are based on rain gauge records through December 2000 (Bonnin et al. 2006). It has been used as an engineering reference to create hypothetical storm scenarios and to develop plans and strategies for storm water management (Chen et al. 2009; Miller et al. 2007). We know, however, that precipitation varies spatially and that single gauge observations may not adequately characterize the *areal* rainfall distribution that drives hydrological processes. Misrepresenting the spatial and temporal variability of precipitation causes runoff model error (Fontaine 1991; Ruelland et al. 2008). For the purpose of flood response, storm water management, and infrastructure design, point-based estimation of IDF needs to be scaled to *areal* estimates to provide more accurate rainfall-runoff model inputs (Nguyen et al. 1981).

The *areal* estimation of IDF can be achieved in two ways. The first way is to convert the point estimates to areal estimates using a converting factor or a ratio. Adopting Areal Reduction Factors (ARF) is one method used to convert point estimates to area-based precipitation exceedance probability. ARF measure the ratio of the mean precipitation across an area to the maximum precipitation depth at a point within it, at a certain duration and recurrence interval (Asquith and Famiglietti 2000). NOAA's *Atlas-14* incorporates this concept. While based on frequency estimates at gauges, it assumes that areal estimates can be produced by averaging the point values at all locations within the area of interest, then multiplying the average by the appropriate ARF (Bonnin et al. 2006). Commonly-used ARF values are documented in US Weather Bureau Technical Report 29 (US Weather Bureau 1957), NOAA Technical Report 24 (Myers and Zehr 1980), NOAA Technical Memorandum HYDRO-40 (Zehr and Myers 1984),

and NOAA *Atlas-2* (Miller et al. 1973). However, these sources have limitations. For example, TP-29 produces a single ARF-area curve for all recurrence intervals (from 2 to 100 years) and implicitly equates the frequency of the point precipitation to the frequency of areal precipitation, assuming that frequency has no influence on the relationship between depth and area (Asquith and Famiglietti 2000). TP-24 attempted to explore the areal and durational variations that were not addressed in TP-29, but it provides ARF only for areas less than 1200 km^2 and storm durations less than or equal to 24 h. These limitations hinder the conversion of point-based estimates into area-based estimates in NOAA's *Atlas-14*.

Spatial analysis techniques and new technology have improved the areal representation of precipitation during the past two decades. In particular, radar-enhanced precipitation estimates have improved ARF calculations and have revealed an inherent overestimation found in previous methods (Lombardo et al. 2006). Additionally, radar data have been vetted to measure explicitly how uncertainties in data quality control on storm duration and area, data heterogeneities, and data record length affect ARF estimation (Durrans et al. 2002; Olivera et al. 2008; Overeem et al. 2010).

Despite efforts to develop and improve ARF calculation (e.g., De Michele et al. 2001; Veneziano and Langousis 2005; Veneziano et al. 2006), the method has been criticized. First, the ARF averaging process obscures information about the spatial and temporal variability of extreme precipitation, factors that strongly influence flood response. Second, the reduction of considerable variability into a single ARF induces uncertainties. Third, ARF generalizes uniformly across a given area, ignoring local or regional extreme rainfall climatology (Wright et al. 2012; Wright et al. 2013).

Recognizing these shortcomings, the second way is to generate IDF *directly* from the products that provide areal representation of precipitation. It involves the creation of areal representation of precipitation and the estimation based on areal precipitation products. The creation of areal representation of precipitation rely on geostatistical methods. These methods which include, but not limit to, the Inverse Distance Weighted (IDW) method, the family of kriging methods (e.g., universal kriging, cokriging and block kriging), sequential Gaussian simulations, have been investigated and applied to various purpose of studies in different regions (e.g., (Liu et al. 2016 ; Park, Kyriakidis, and Hong 2017 ; Park et al. 2016 ; Gundogdu 2017)). Meanwhile, the integration of radar technology and geostatistical methods has greatly improved the accuracy of areal representation of precipitation (Cecinati et al. 2017). Particularly, the gridded PRISM (Parameter-elevation Relationships on Independent Slopes Model) data, the official spatial climate data sets of the U.S. Department of Agriculture, have been producd using methods that consider location, elevation, coastal proximity, topographic facet orientation, vertical atmospheric layer, topographic position, and orographic effectiveness of the terrain and incorporate radar observations. The uncerntainty of PRISM data has also been rigously assessed (Daly et al. 2008).

Wright et al. (2013)'s work exemplifies the usage of radar data to generate the areal estimation of IDF. They built "storm catalogs" from a 10-year high-resolution radar database and developed the Stochastic Storm Transposition (SST) method which resamples from storm catalogs to reconstruct a regional climatology of extreme rainfall. They applied their method to reproduce IDFs for four watersheds around Charlotte, North Carolina and revealed substantial variability that could not be captured by conventional methods, but which has great implications to flood risk management. Their work provided an alternative way to construct areally-based

IDFs directly from real storms by taking the advantage of high resolution of gridded precipitation products which capture variabilities of extreme rainfall and regional extreme rainfall climatology, instead of using generalized ARF to convert point-based estimates into area-based estimates. Meanwhile, their work also highlighted the idea of Regional Frequency Analysis (RFA) which substitutes space for time by using samples from other locations that have similar extreme statistical probabilities to make reliable statistical inferencing. RFA is a typical way of overcoming the problem of insufficient sample size in the study of hydrometeorology extremes (Kysely and Picek 2007; Wallis 1980, 1982; Weiss and Bernardara 2013) and is also used in the establishment of *Atlas-14* (Bonnin et al. 2006). However, their work only focused on a single region (i.e., Charlotte, North Carolina) and storms with durations up to 12 hours.

The losses caused by recent heavy rainfall and flooding events in the United States, and the potential for intensified extreme precipitation in the future, motivate this study to examine precipitation extremes at the basin level using a spatially-explicit and regionally-coherent model. We present an approach to estimate exceedance probability of total precipitation received in differently-sized United States Geological Survey (USGS) Hydrologic Units taking the advantage of PRISM data which provide daily total precipitation in the continental United States from 1 January 1981 up to present as we discussed above. Our approach includes a regionalization method that delineates regions to capture different extreme rainfall climatology across space and a resampling scheme that substitutes space for time taking advantage of a high-resolution, areally-representative data set. We tested our methods and compared against the point-based approach adopted by NOAA's *Atlas-14* by examining IDFs in selected basins impacted by recent heavy rainfall and flooding events in South Carolina, West Virginia, Texas,

Louisiana, Colorado, Washington, Oregon, and Idaho. These states were selected to represent areas across the US that have recently experienced heavy rainfall and flooding events.

Methods

Overview

To examine the probability of occurrence of a heavy precipitation event in an area, such as on of USGS's 10-digit or 8-digit Hydrologic Unit Codes (HUCs), the annual maximum total precipitation was extracted from the daily 4-km gridded PRISM precipitation dataset covering the period, 1 January 1981 to present (PRISM Climate Group, Oregon State University, http://prism.oregonstate.edu, created 4 Feb 2004). Total rainfall in the sampled area was calculated by summing consecutive 1-, 2-, and 4-day totals of all grid cells within the hydrologic unit, for each year from 1 January 1981 through 31 December 2015. Thirty five years of annual maxima are insufficient for robust estimation of Generalized Extreme Value (GEV) distribution parameters, especially when estimating long return periods. We adopt the idea of Regional Frequency Analysis (RFA) which finds more samples from other locations that have similar extreme statistical probabilities to make reliable statistical inferencing. We developed a bootstrapping approach that samples spatially across regions with relatively homogeneous extreme value statistical properties. In this sense, it substitutes space for time, compensating for the relatively short period of record when accounting for extreme events. One-, two-, and four-day annual maximum total precipitation values were sampled across a broader region where conditions causing heavy precipitation events plausibly could have occurred because of similar geographic and synoptic conditions. Thus, we used the size and shape of the original watershed to randomly stamp identical polygons across region to generate a large sample. This sample provides the basis for estimation of GEV curves and event probability based on the areal

158 precipitation total in the resampled basins. Finally, we compared the area-based estimates against
159 the point-based estimates from *Atlas-14*.

160 *Heavy rainfall events and watersheds*

161 We examined five recent heavy rainfall events across the United States. For each event,
162 we selected the most impacted HUC 8 or HUC10 watersheds that have rain gauges within them
163 (Table 1). Among them, Gills Creek, in central South Carolina, had five dam failures within the
164 watershed during the recent flooding. We seek to explore how probability of occurrence changes
165 for basins vs. points.

166

167 *Regionalization*

168 We employed a regionalization method named REDCAP (Regionalization with
169 Dynamically Constrained Agglomerative Clustering And Partitioning; Guo, 2008) to delimit
170 homogenous regions with relatively homogenous annual maximum 1-day, 2-day, and 4-day
171 rainfall statistical properties separately from PRISM. For each grid cell in PRISM, we extracted
172 annual maximum 1-day, 2-day, and 4-day rainfall totals. The dissimilarity of the pairwise grid
173 cells was defined by the Anderson-Darling (AD) distance for annual maximum 1-day, 2-day, and
174 4-day rainfall totals from 1981 to 2015. This method disproportionately weights observations in
175 the tails of the distribution (Anderson and Darling 1954; Pettitt 1976). It is chosen because it is
176 one of the metrics used to form homogeneous regions for the growth curves in Regional
177 Frequency Analysis (RFA) (Viglione et al. 2007) and has also been used in the regionalization of
178 heavy precipitation (Gao et al. 2016).

REDCAP finds sets of grid cells that are spatially contiguous and have the shortest AD distance among them. At the beginning, REDCAP considers each grid cell as an individual cluster. Then, it iteratively merges pairs of clusters that are spatially contiguous and have the shortest AD distance, which is determined as the averaged distance of each pair of grid cells across the two merged clusters. This follows the same clustering procedure as conventional average linkage clustering except that REDCAP requires that merged cluster pairs be spatially contiguous. A spatially contiguous dendrogram is constructed once all grid cells are merged. REDCAP then partitions the spatially contiguous dendrogram into the desired number of sub-trees assigned by a user, each of which represents a spatially contiguous region (Figure 2). At each cutting of the dendrogram, REDCAP minimizes the sum of within-region heterogeneity for all regions which is defined as:

$$H = \sum_{i}^{n} \sum_{j}^{m} AD_{(i,j)}$$

where, H is the sum of within-region heterogeneity for n regions, m is the number of grid cells in region i, and $AD_{(i,j)}$ is the averaged AD distance of cell j to the other $(m-1)$ cells within the region i. The number of sub-trees (i.e., regions) was determined on the basis of *prior* knowledge of climate regions and consideration for geographic and synoptic conditions of the target watersheds (Figure 1a to 1c).

Bootstrap sampling and probability estimation

For each selected 8-digit HUC watershed, a layer that contains 30 non-overlapping polygons that have the same shape and area as the selected watershed was generated in each year from 1981 to 2015. Regions were determined on the basis of 1-day, 2-day, or 4-day totals

delineated by REDCAP (Figure 1 and Table 1). Only 1-day and 2-day totals were investigated for Gauley (WV), because the event was concentrated in two days. Twenty bootstrap samples were taken for the 1-day total precipitation of Gauley due to the small size of region 1 (Figure 1a). Thirty samples were taken from both region 4 and 5 for the 4-day total of Cooper (SC), because the watershed is split equally across these two regions (Figure 1c). The same approach was applied to 10-digit HUCs (i.e., Gills Creek) to create a layer of 100 sample areas in each year. The annual maximum of 1-day, 2-day, and 4-day totals were extracted from these randomly created polygons. Total rainfall depth in each watershed was standardized by the number of PRISM grid cells within the watershed (i.e., the average rainfall depth of each grid cell) to facilitate comparison with observations at weather stations. In this way, additional samples were created to estimate GEV parameters. This method substitutes space for time, to account for the limited period of record (Viglione et al. 2007; Wallis 1980, 1982).

The annual maxima from the two datasets were used together to fit GEV curves. The location, scale, and shape parameters of the GEV distribution and the intensity of 2-, 5-, 10-, 25-, 50-, 100-, 200-, 400-, 600-, 800-, and 1000-year return periods in each watershed were estimated using L-moments (Hosking and Wallis 2005). The terminology of exceedance probabilities in the study of the Great Colorado Flood of September 2013 was used to represent the probabilities corresponding to each return period (e.g., a 500 year event has a exceedance probability of 0.002 (1/500)) (Gochis et al. 2015). A lower exceedance probability suggests a longer return period or smaller probability rainfall event. To avoid the bias that might be caused by randomness of generating the layers, the procedure was repeated ten times by permutating the layers used for sampling in each year. GEV curves were fitted using annual maxima extracted from the randomly created datasets and the selected watersheds each time. The intensity at each

recurrence interval was averaged across the ten sample sets. Root Mean Square Error (RMSE) at each recurrence interval of the ten sample sets was used to examine the variation of the sample sets.

Comparison with the point-based approach

The comparison of the area- and point-based approaches were conducted in two ways. The first comparison is the estimated rainfall depths of 1-, 2-, and 4-day totals at recurrence intervals of 50, 100, 200, 500, and 1000 years. In each selected watershed, we compared the area-based estimates of rainfall depths against the maximum estimated rainfall depths of *Atlas-14* grid cells in each watershed. The ratio of these two are analogous to ARF which is used to convert point-based values to area-based estimates. The difference of these ratios across watersheds and duration periods suggests that no universal ARF sufficiently characterizes the point to area relationship. In addition, ARF is only applicable to watersheds smaller than 1200 km^2 and storm durations shorter than or equal to 24 hours (Myers and Zehr 1980; Zehr and Myers 1984). The second comparison is the exceedance probability of the investigated heavy rainfall events suggested by the area- vs. point-based approaches. The area-based exceedance probability was estimated by comparing observed rainfall depth within the watershed during these heavy rainfall events against the estimated intensity at each recurrence interval. Similarly, the point-based exceedance probability was estimated by comparing the observed rainfall depth at individual weather stations against the intensity at each recurrence interval provided by NOAA's *Atlas-14*. The comparisons could not be conducted in one basin (Wilson-Trusk-Nestuccu, OR), because NOAA's *Atlas-14* has not been updated in Oregon since 1973.

Results

Gridded 1-, 2-, and 4- day totals from PRISM exhibited great spatial variability within watersheds (colored pixels in Figure 3 to 8). The ratio of the maximum to minimum grid cell value was greatest in St. Vrain for 1-day total precipitation (Figure 4b, 11.4 (168.5 mm / 14.8 mm)). The minimum ratio was about 1.4 in Saline Bayou for both 2-day and 4-day totals (Figure 7c and 7d). The density and spatial arrangement of rain gauges also differed greatly across watersheds (black dots and stars in Figure 3 to 8). When the density of gauges in a watershed was relatively high and distributed across the entire watershed, such as in the St. Vrain (Figure 4) and Cooper basins (Figure 5), they captured both high and low rainfall extremes. The sparse density and distribution of rain gauges did not fully capture the spatial variability of rainfall patterns within watersheds such as Gills Creek (Figure 6), Saline Bayou (Figure 7), and Gauley (Figure 8).

The spatial variability of rainfall and the spatial arrangement of rain gauges produced different exceedance probabilities for each individual station within a basin (Table 2). The exceedance probability suggested by a single rain gauge cannot represent the exceedance probability across a basin. For example, 93 gauges in St. Vrain suggested six different levels of exceedance probability for 2- and 4-day totals (Figure 4b and 4c; Table 2). To facilitate interpretation, our comparison focuses on the lowest exceedance probability suggested by the point-based approach against that estimated by the area-based approach. Except for the 1-day total in St. Vrain and 1- and 2-day totals in Gauley, the area-based resampling approach estimated lower exceedance probabilities than those estimated by the point-based approach (Figure 3 to 8; Table 2). The most distinguishable difference occurred in Gills Creek. The area-based approach estimated an event with probability lower than 0.1% (greater than a 1000-year

267 event) for 1-, 2-, and 4-day totals, while the point-based approach estimated a probability of 0.1-
268 0.2% or a 500- to 1000-year event (Figure 6b to 6d).

269 The area-based estimates of 1-, 2-, and 4-day total rainfall depths at different recurrence
270 intervals had good convergence. The majority of RMSE were lower than 10 mm (Table 3). The
271 comparison of the estimated rainfall depths suggested by the point- and area-based methods
272 further explained the different exceedance probabilities suggested by the two approaches. The
273 largest difference (i.e., the lowest ratio of area- to point-based) was associated with 1-day total
274 precipitation in the St. Vrain Basin, while the smallest difference was associated with 4-day total
275 precipitation in the Cooper Basin (Figure 9). The ratio of area- to point-based estimates varied
276 both among watersheds and across different durations in the same watershed. Many factors such
277 as regional climatology and watershed characteristics (e.g., area, shape, and geographic location)
278 could contribute to the difference among watersheds. The ratio tended to decrease as return
279 periods increased, with the exception of 1- and 2-day totals in Gauley and 2- and 4-day totals in
280 Cooper. Within a watershed, the ratio decreased as duration increased from 1 day to 4 days.
281 Because short-duration storms tend to be more localized, they likely caused greater difference
282 between rainfall depth at a single location relative to the greater area than long-duration storms
283 with more widespread, uniform precipitation patterns over a large space.

284 **Discussion and Summary**

285 The difference between the heavy rainfall exceedance probabilities estimated by the
286 point- and area-based approaches are expected. While they are based on the same statistical
287 properties of heavy rainfall, they are investigated at different spatial scales. One does not
288 substitute for the other. Point-based estimates are usually derived from rain gauge observations
289 that are often the most accurate source of rainfall data and may be available for sufficiently long

periods (Willems 2012). This makes the point-based estimates such as *Atlas-14* very useful as an engineering standard.

However, some engineering practices (e.g., the design of hydraulic structures), require knowledge of how much rain is likely to be received across an *area* (Svensson and Jones 2010). A point-based approach identifies maximum precipitation for points without a specific areal extent, and it is very challenging to scale from point-based estimates to area-based estimates. One cannot simply extrapolate from single points to obtain areal estimates, because probability estimates at each point represent that point *without* a clearly defined spatial extent. The two typical upscaling methods – design storms and ARF have recognized shortcomings. The former makes unrealistic assumptions about uniformity of rainfall across space and time. The latter ignores spatial and temporal variability (Svensson and Jones 2010; Wright et al. 2012).

To estimate the area-based heavy rainfall exceedance probabilities, our approach takes advantage of areal representation of precipitation from high-resolution, gridded PRISM (Daly et al. 2008) that has been used to investigate precipitation patterns (Lundquist et al. 2015), to measure vegetation response to climate stresses (Canon et al. 2011), and to estimate discharge in watersheds (Golden et al. 2010). Besides this advantage, our methods have several other merits.

First, we recognize climatological homogeneity of heavy rainfall exceedance probabilities using a regionalization approach that is objective, data driven, and tailored to extreme rainfall at different durations. By resampling within objectively delineated regions, we differentiated geographic and synoptic conditions that contribute to heavy rainfall in specific regions.

311 Second, by delineating homogeneous regions on the basis of extreme statistical properties
312 we can "substitute space for time" and significantly increase sample size, making statistical
313 inferences more robust. In spirit, this is similar to Regional Frequency Analysis (RFA) adopted
314 by *Atlas-14* which borrows from stations with similar extreme value properties to estimate
315 station probabilities (Hosking and Wallis 2005). Our regionalization method delimited not only
316 homogenous, but spatially contiguous regions that enabled the resampling of continuous areas
317 (i.e., watersheds) rather than discrete precipitation grid cells.

318 Third, our resampling approach sampled real events with spatial and temporal
319 characteristics, rather than relying on unrealistic assumptions about spatial rainfall patterns. It
320 offered an opportunity to examine truly plausible outcomes, ones that already occurred. This is a
321 way of more fully sampling the record of actual storm events in a coherent, internally consistent
322 spatial and temporal sense.

323 Fourth, although 35 years of gridded precipitation data (i.e., 1981-2015) is short in terms
324 of long return periods, and as compared to observational records at some individual rain gauges,
325 sampling from the most recent period reduces problems associated with non-stationarity. The
326 increasing trend of extreme precipitation events has been observed in the eastern and Midwest of
327 United States (Easterling et al. 2000; Todd et al. 2006). Non-stationarity in the record makes the
328 most recent 35 years more relevant.

329 The difference between the heavy rainfall exceedance probabilities estimated by the
330 point- and area-based approaches has several implications. First, as suggested by other studies,
331 generalized ARF are limited when applied to all watersheds without considering local and
332 regional extreme rainfall climatology (Asquith and Famiglietti 2000; Durrans et al. 2002; Wright

et al. 2012). Second, given the dam failures in Gills Creek, it is very likely that the area-based approach more appropriately measured the severity of the event. In most of the examples we investigated, the area-based approach suggested lower exceedance probabilities than the point-based approach. This suggests that severe heavy rainfall events could have happened more often than would have been estimated by a point-based approach. Our results suggest that point-based estimates (even with point-to-areal conversion) should be used cautiously as model inputs.

Likewise, gridded precipitation products have their own shortcomings. For example, PRISM data have no durations shorter than 24 hours, result from uneven station networks, and use spatial interpolation (Daly et al., 2008). However, our method provides the basis for use with ever-improving gridded precipitation data. Ultimately, the use of gridded data as input for hydrologic modeling or infrastructure design requires its own performance evaluation.

In summary, our study shows considerable difference between the point- and area-based estimates of heavy rainfall exceedance probabilities and IDF curves in the selected watersheds impacted by five recent heavy rainfall and flooding events in the continental United States. The area-based estimates, when coupled with hydrological models, have important implications to storm water management and flood risk assessment.

Acknowledgements

This research was partially supported by the National Oceanic and Atmospheric Administration (NOAA) Climate Program Office (grant no. NA11OAR4310148 and NA16OAR4310163) to the Carolinas Integrated Sciences and Assessments and partly based on work funded by NSF grant no. 0748813.

References

Anderson, T. W., and D. A. Darling. (1954). "A Test of Goodness of Fit." *Journal of the American Statistical Association,* 49, 765-769.

Asquith, W., and J. Famiglietti. (2000). "Precipitation areal-reduction factor estimation using an annual-maxima centered approach." *Journal of Hydrology*, 230, 55-69.

Bonnin, G. M., D. Martin, B. Lin, T. Parzybok, M. Yekta, and D. Riley. (2006). "Precipitation-frequency atlas of the United States." *NOAA atlas*, 14 Volume 2 Version 3.0, 1-65 .

US Weather Bureau, 1957. Rainfall intensity–frequency regime 1.The Ohio valley; 2. Southeastern United States. Tech. Paper No. 29, US Department of Commerce, Washington DC, 1957.

Cecinati, F., M. A. Rico-Ramirez, G. B. Heuvelink and D. Han. (2017). "Representing radar rainfall uncertainty with ensembles based on a time-variant geostatistical error modelling approach." *Journal of Hydrology*, 548, 391-405.

Canon, J., F. Dominguez, and J. B. Valdes. (2011). "Vegetation responses to precipitation and temperature: a spatiotemporal analysis of ecoregions in the Colorado River Basin." *International Journal of Remote Sensing*, 32, 5665-5687.

Chen, J., A. A. Hill, and L. D. Urbano. (2009). "A GIS-based model for urban flood inundation." *Journal of Hydrology,* 373, 184-192.

Daly, C., M. Halbleib, J. I. Smith, W. P. Gibson, M. K. Doggett, G. H. Taylor, J. Curtis, and P. P. Pasteris. (2008). "Physiographically sensitive mapping of climatological temperature and precipitation across the conterminous United States." *International Journal of Climatology*, 28, 2031-2064.

De Michele, C., N. T. Kottegoda, and R. Rosso. (2001). "The derivation of areal reduction factor of storm rainfall from its scaling properties." *Water Resources Research,* 37, 3247-3252.

Durrans, S. R., L. T. Julian, and M. Yekta. (2002). "Estimation of depth-area relationships using radar-rainfall data." *Journal of Hydrologic Engineering,* 7, 356-367.

Dyrrdal, A. V., T. Skaugen, F. Stordal, and E. J. Forland. (2016). "Estimating extreme areal precipitation in Norway from a gridded dataset." *Hydrological Sciences Journal-Journal Des Sciences Hydrologiques,* 61, 483-494.

Easterling, D. R., J. L. Evans, P. Y. Groisman, T. R. Karl, K. E. Kunkel, and P. Ambenje. (2000). "Observed variability and trends in extreme climate events: A brief review." *Bulletin of the American Meteorological Society,* 81, 417-425.

Federal Emergency Management Agency. (2017). “Significant Flood Events”, https://www.fema.gov/significant-flood-events, last access on May 30, 2017.

Fontaine, T. A. (1991). "Predicting Measurement Error of Areal Mean Precipitation during Extreme Events." *Water Resources Bulletin,* 27, 509-520.

Gao, P., G. J. Carbone, and D. Guo. (2016). "Assessment of NARCCAP model in simulating rainfall extremes using a spatially constrained regionalization method." *International Journal of Climatology*, 36 (5), 2368 - 2378.

Gochis, D., R. Schumacher, K. Friedrich, N. Doesken, M. Kelsch, J. Z. Sun, K. Ikeda, D. Lindsey, A. Wood, B. Dolan, S. Matrosov, A. Newman, K. Mahoney, S. Rutledge, R. Johnson, P. Kucera, P. Kennedy, D. Sempere-Torres, M. Steiner, R. Roberts, J. Wilson, W. Yu, V. Chandrasekar, R. Rasmussen, A. Anderson, and B. Brown. (2015). "The Great Colorado Flood of September 2013." *Bulletin of the American Meteorological Society,* 96, 1461-1487.

Golden, H. E., C. D. Knightes, E. J. Cooter, R. L. Dennis, R. C. Gilliam, and K. M. Foley. (2010). "Linking air quality and watershed models for environmental assessments: Analysis of the effects of model-specific precipitation estimates on calculated water flux." *Environmental Modelling & Software*, 25, 1722-1737.

Gundogdu, I. B. (2017). "Usage of multivariate geostatistics in interpolation processes for meteorological precipitation maps." *Theoretical and Applied Climatology*, 127, 81-86.

Guo, D. (2008). "Regionalization with dynamically constrained agglomerative clustering and partitioning (REDCAP)." *International Journal of Geographical Information Science*, 22, 801-823.

Guttman, N. B. (1993). "The Use of L-Moments in the Determination of Regional Precipitation Climates." *Journal of Climate*, 6, 2309-2325.

Hosking, J. R. M., and J. R. Wallis. (2005). *Regional frequency analysis: an approach based on L-moments*, Cambridge, United Kingdom: Cambridge University Press.

Kysely, J., and J. Picek. (2007). "Regional growth curves and improved design value estimates of extreme precipitation events in the Czech Republic." *Climate Research*, 33, 243-255.

Liu, Y., S. Hu, D. Sheng, L. Chang and M. Jia. (2016). "Study of precipitation interpolation at Xiangjiang River Basin based on Geostatistical Analyst." In *Geoinformatics, 2016 24th International Conference on*, 1-5, edited., IEEE.

Lombardo, F., F. Napolitano, and F. Russo. (2006). "On the use of radar reflectivity for estimation of the areal reduction factor." *Natural Hazards and Earth System Sciences*, 6, 377-386.

Lundquist, J. D., M. Hughes, B. Henn, E. D. Gutmann, B. Livneh, J. Dozier, and P. Neiman. (2015). "High-Elevation Precipitation Patterns: Using Snow Measurements to Assess

Daily Gridded Datasets across the Sierra Nevada, California." *Journal of Hydrometeorology*, 16, 1773-1792.

Mailhot, A., S. Duchesne, D. Caya and G. Talbot. (2007). "Assessment of future change in intensity-duration-frequency (IDF) curves for southern Quebec using the Canadian regional climate model (CRCM)." *Journal of Hydrology*, 347, 197-210.

Merz, B., H. Kreibich, R. Schwarze, and A. Thieken. (2010). "Review article 'Assessment of economic flood damage'." *Natural Hazards and Earth System Sciences*, 10, 1697-1724.

Miller, J., R. Frederick, and R. Tracey. (1973). " Precipitation-frequency atlas of the conterminous western United States (by states) NOAA Atlas 2", http://www.nws.noaa.gov/oh/hdsc/currentpf.htm, last access on May 30, 2017.

Miller, S. N., D. J. Semmens, D. C. Goodrich, M. Hernandez, R. C. Miller, W. G. Kepner, and D. P. Guertin. (2007). "The Automated Geospatial Watershed Assessment tool." *Environmental Modelling & Software*, 22, 365-377.

Mirhosseini, G., P. Srivastava and L. Stefanova. (2013). "The impact of climate change on rainfall Intensity–Duration–Frequency (IDF) curves in Alabama." *Regional Environmental Change*, 13, 25-33.

Myers, V. A., and R. M. Zehr. (1980). "A methodology for point-to-area rainfall frequency ratios." *National Oceanic and Atmospheric Administration Technical Report NWS 24*, http://www.nws.noaa.gov/oh/hdsc/Technical_reports/TR24.pdf, last access on May 30, 2017.

National Weather Service. (2016). "Hydrologic Information Center - Flood Loss Data" http://www.nws.noaa.gov/hic/, last access on May 30, 2017.

445 Nguyen, V. T. V., J. Rousselle, and M. B. Mcpherson. (1981). "Evaluation of Areal Versus Point
446 Rainfall with Sparse Data." *Canadian Journal of Civil Engineering,* 8, 173-178.
447 Olivera, F., J. Choi, D. Kim, and M. H. Li. (2008). "Estimation of average rainfall areal
448 reduction factors in Texas using NEXRAD data." *Journal of Hydrologic Engineering,* 13,
449 438-448.
450 Overeem, A., T. A. Buishand, I. Holleman, and R. Uijlenhoet. (2010). "Extreme value modeling
451 of areal rainfall from weather radar." *Water Resources Research,* 46, W09514.
452 Park, N.-W., S. Hong, P. C. Kyriakidis, W. Lee and S.-J. Lyu. (2016). "Geostatistical
453 downscaling of AMSR2 precipitation with COMS infrared observations." *International*
454 *Journal of Remote Sensing,* 37, 3858-3869.
455 Park, N.-W., P. C. Kyriakidis and S. Hong. (2017). "Geostatistical Integration of Coarse
456 Resolution Satellite Precipitation Products and Rain Gauge Data to Map Precipitation at
457 Fine Spatial Resolutions." *Remote Sensing,* 9, 255.
458 Peck, A., P. Prodanovic and S. P. Simonovic. (2012). "Rainfall Intensity Duration Frequency
459 Curves Under Climate Change: City of London, Ontario, Canada." *Canadian Water*
460 *Resources Journal,* 37, 177-189.
461 Pettitt, A. N. (1976). "A two-sample Anderson-Darling rank statistic." *Biometrika,* 63, 161-168.
462 Ruelland, D., S. Ardoin-Bardin, G. Billen, and E. Servat. (2008). "Sensitivity of a lumped and
463 semi-distributed hydrological model to several methods of rainfall interpolation on a
464 large basin in West Africa." *Journal of Hydrology,* 361, 96-117.
465 SC Department of Health and Environmental Control. (2017). “2015 S.C. Flood Dam Response
466 and Recovery”,

http://www.scdhec.gov/HomeAndEnvironment/DisasterPreparedness/FloodUpdates/, last access on May 30, 2017.

Soltani, S., R. Helfi, P. Almasi and R. Modarres. (2017). "Regionalization of Rainfall Intensity-Duration-Frequency using a Simple Scaling Model." *Water Resources Management*,4253-4273.

Svensson, C., and D. A. Jones. (2010). "Review of methods for deriving areal reduction factors." *Journal of Flood Risk Management,* 3, 232-245.

Todd, C. E. D., J. M. Harbor, and B. Tyner. (2006). "Increasing magnitudes and frequencies of extreme precipitation events used for hydraulic analysis in the Midwest." *Journal of Soil and Water Conservation,* 61, 179-185.

Veneziano, D., and A. Langousis. (2005). "The areal reduction factor: A multifractal analysis." *Water Resources Research,* 41, W07008.

Veneziano, D., A. Langousis, and P. Furcolo. (2006). "Multifractality and rainfall extremes: A review." *Water Resources Research,* 42, W06D15.

Viglione, A., F. Laio, and P. Claps. (2007). "A comparison of homogeneity tests for regional frequency analysis." *Water Resources Research,* 43, W03428.

Wallis, J. (1980). "Risk and uncertainties in the evaluation of flood events for the design of hydraulic structures, Piene e Siccità E." *Guggino, G. Rossi, E. Todini*, 3-36.

Wallis, J. (1982). "Probable and improbable rainfall in California." *Res. Rep. RC,* 9350, 41172.

Willems, P. (2012). *Impacts of climate change on rainfall extremes and urban drainage systems,* London, United Kingdom: IWA Publishing.

Willems, P., K. Arnbjerg-Nielsen, J. Olsson and V. T. V. Nguyen. (2012). "Climate change impact assessment on urban rainfall extremes and urban drainage: Methods and shortcomings." *Atmospheric Research*, 103, 106-118.

Wright, D., J. Smith, G. Villarini, and M. Baeck. (2012). "Applications of radar-based rainfall estimates for urban flood studies." *Pragmatic Modeling of Urban Water Systems, Monograph,* 21, 85-110.

Wright, D. B., J. A. Smith, G. Villarini, and M. L. Baeck. (2013). "Estimating the frequency of extreme rainfall using weather radar and stochastic storm transposition." *Journal of Hydrology*, 488, 150-165.

Zehr, R. M., and V. A. Myers. (1984). "Depth-area ratios in the semi-arid southwest United States." *NOAA Tech. Memo. HYDRO-40,* http://www.nws.noaa.gov/oh/hdsc/PF_related_studies/TechnicalMemorandum_HYDRO40.pdf, last access on May 30, 2017.

Zhu, J. (2013). "Impact of Climate Change on Extreme Rainfall across the United States." *Journal of Hydrologic Engineering*, 18, 1301-1309.

Zhu, J., W. Forsee, R. Schumer and M. Gautam. (2013). "Future projections and uncertainty assessment of extreme rainfall intensity in the United States from an ensemble of climate models." *Climatic Change*, 118, 469-485.

List of Figures

Figure 5 Exceedance probability of October, 2015 heavy rainfall event in Cooper Watershed South Carolina. (a) the location of Cooper; (b) – (d) comparison of exceedance probability estimated by point-based and area-based approaches respectively for 1-, 2-, and 4-day total precipitation.

Figure 6 Exceedance probability of October, 2015 heavy rainfall event in Gills Creek Watershed South Carolina. (a) the location of Gills Creek; (b) – (d) comparison of exceedance probability estimated by point-based and area-based approaches respectively for 1-, 2-, and 4-day total precipitation.

Figure 7 Exceedance probability of March, 2016 heavy rainfall event in Saline Bayou Watershed Louisiana. (a) the location of Saline Bayou; (b) – (d) comparison of exceedance probability estimated by point-based and area-based approaches respectively for 1-, 2-, and 4-day total precipitation.

Figure 8 Exceedance probability of June, 2016 heavy rainfall event in Gauley Watershed West Virginia. (a) the location of Gauley; (b) – (c) comparison of exceedance probability estimated by point-based and area-based approaches respectively for 1- and 2- day total precipitation.

Figure 9 The comparison of the estimated rainfall depths of 1-, 2-, and 4-day totals at recurrence intervals of 50, 100, 200, 500, and 1,000 years from the point-based and area-based approaches. The values of the point-based approach are the maximum estimated rainfall depths of *Atlas-14* grids within a watershed. The ratios are the depths suggested by the area-based approach to the maximum depth estimated by the point-based approach.


(a)
(b)
(c)
(d)
1
2
3
4
5
6
N
0 250 500 1,000 1,500
km
Gills Creek
Bootstrap Smaples
0 250 500 1,000
km

Figure 1

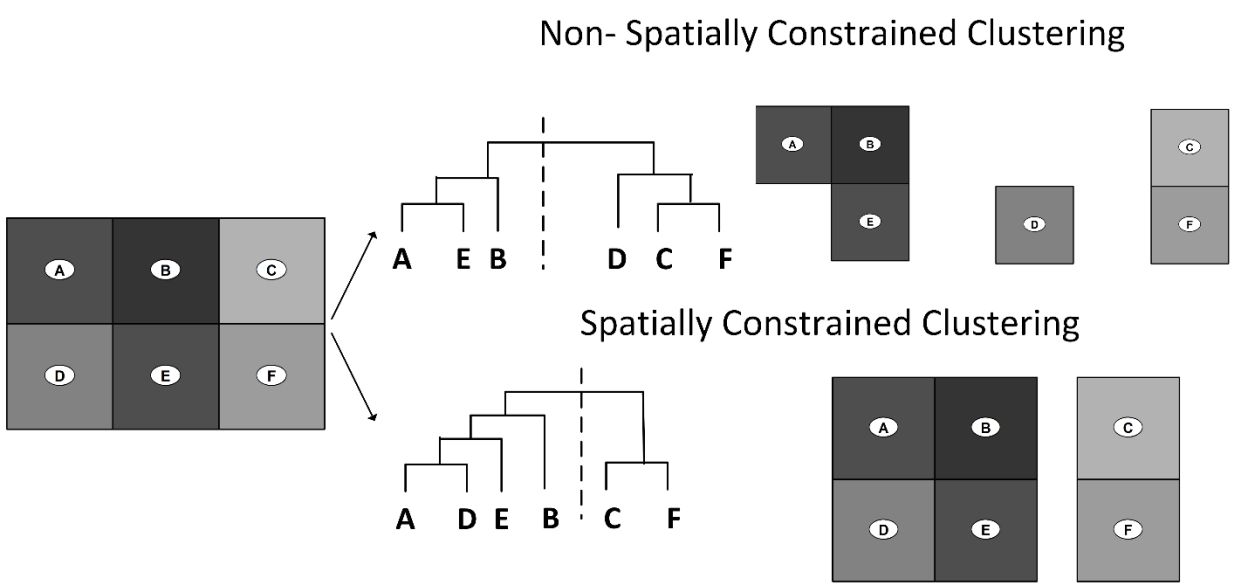
Non- Spatially Constrained Clustering
A
B
C
D
E
F
A E B D C F
A
B
E
D
C
F
Spatially Constrained Clustering
A D E B C F
A
B
C
D
E
F

Figure 2

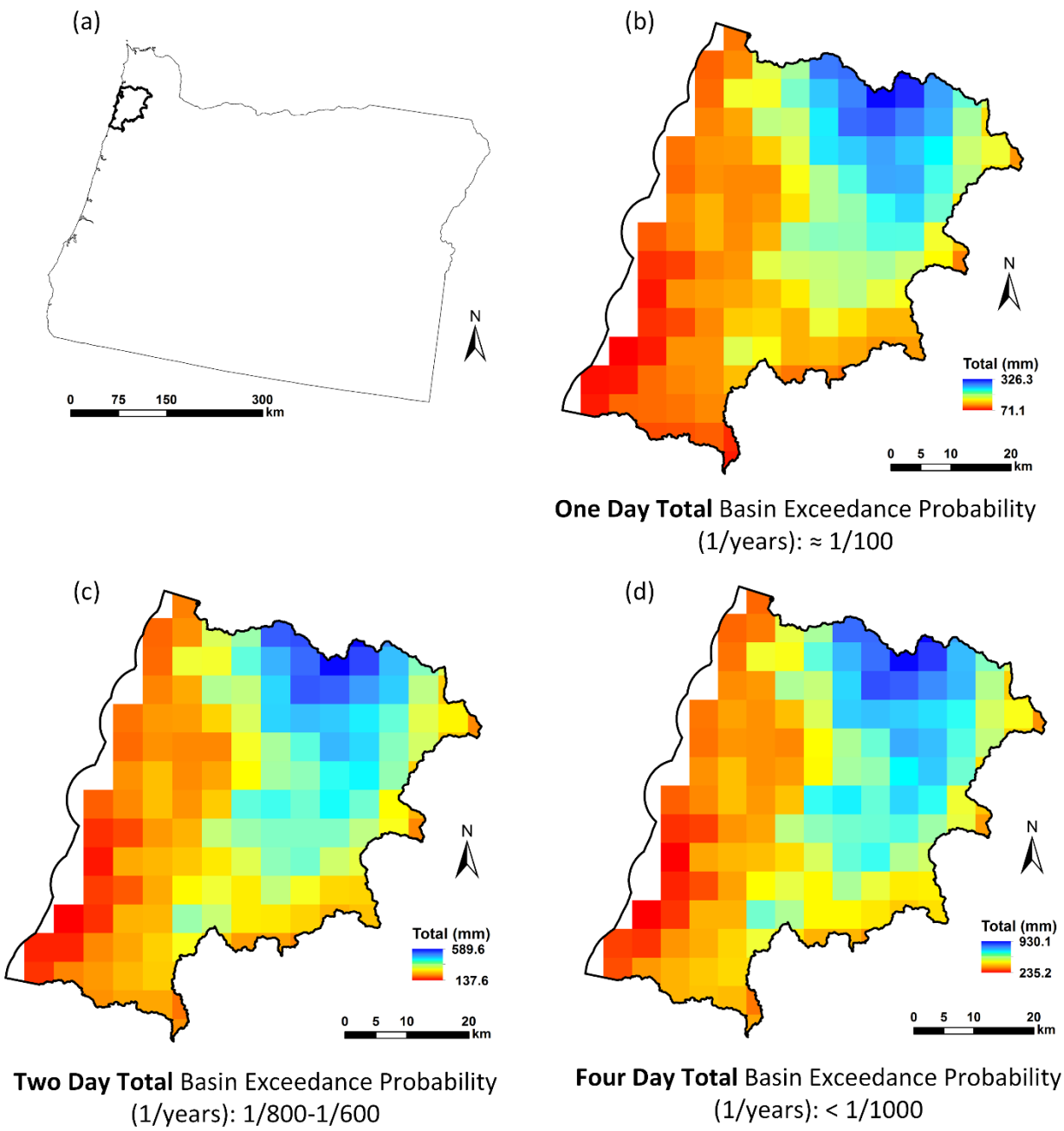
(a)
N
0 75 150 300
km
(b)
N
Total (mm)
326.3
71.1
0 5 10 20
km
One Day Total Basin Exceedance Probability
(1/years): ≈ 1/100
(c)
N
Total (mm)
589.6
137.6
0 5 10 20
km
Two Day Total Basin Exceedance Probability
(1/years): 1/800-1/600
(d)
N
Total (mm)
930.1
235.2
0 5 10 20
km
Four Day Total Basin Exceedance Probability
(1/years): < 1/1000

Figure 3

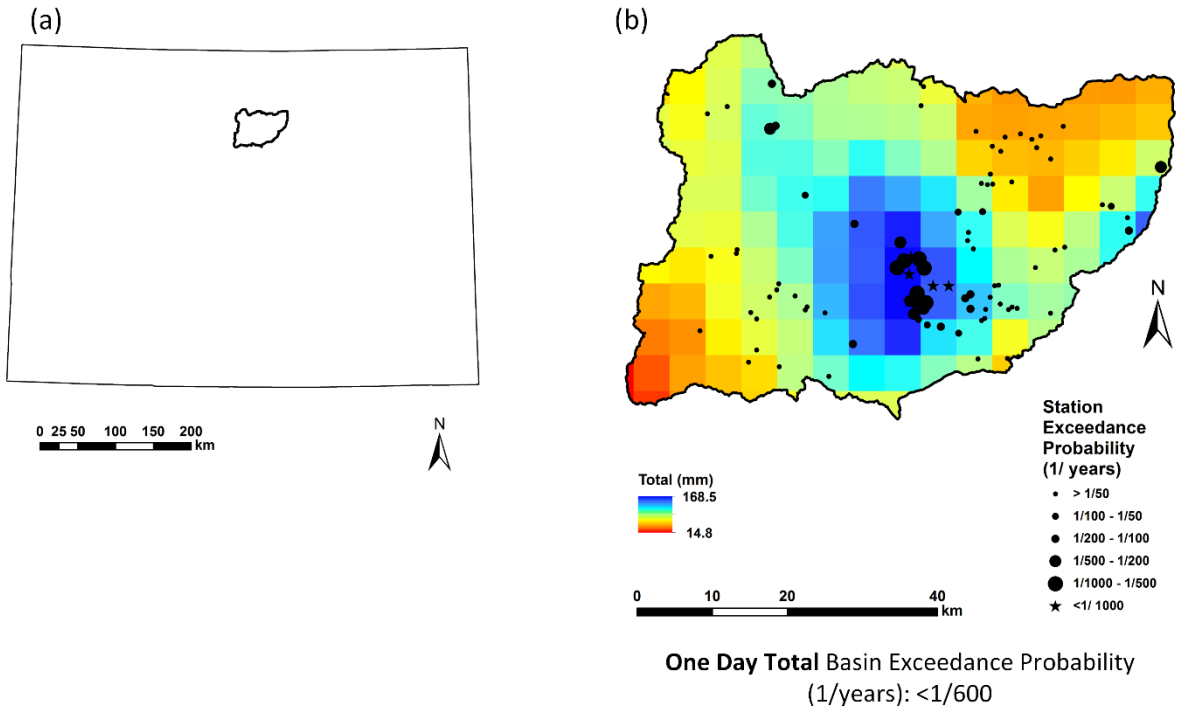
(a)
0 25 50 100 150 200
km
N
(b)
N
Total (mm)
168.5
14.8
0 10 20 40
km
Station Exceedance Probability (1/ years)
> 1/50
1/100 - 1/50
1/200 - 1/100
1/500 - 1/200
1/1000 - 1/500
<1/ 1000
One Day Total Basin Exceedance Probability (1/years): <1/600
(c)
N
Total (mm)
278.0
41.4
0 10 20 40
km
Station Exceedance Probability (1/ years)
> 1/50
1/100 - 1/50
1/200 - 1/100
1/500 - 1/200
1/1000 - 1/500
<1/ 1000
Two Day Total Basin Exceedance Probability (1/years): < 1/1000
(d)
N
Total (mm)
337.1
74.5
0 10 20 40
km
Station Exceedance Probability (1/ years)
> 1/ 50
1/100 - 1/50
1/200 - 1/100
1/500 - 1/200
1/1000 - 1/500
< 1/ 1000
Four Day Total Basin Exceedance Probability (1/years): <1/1000

Figure 4

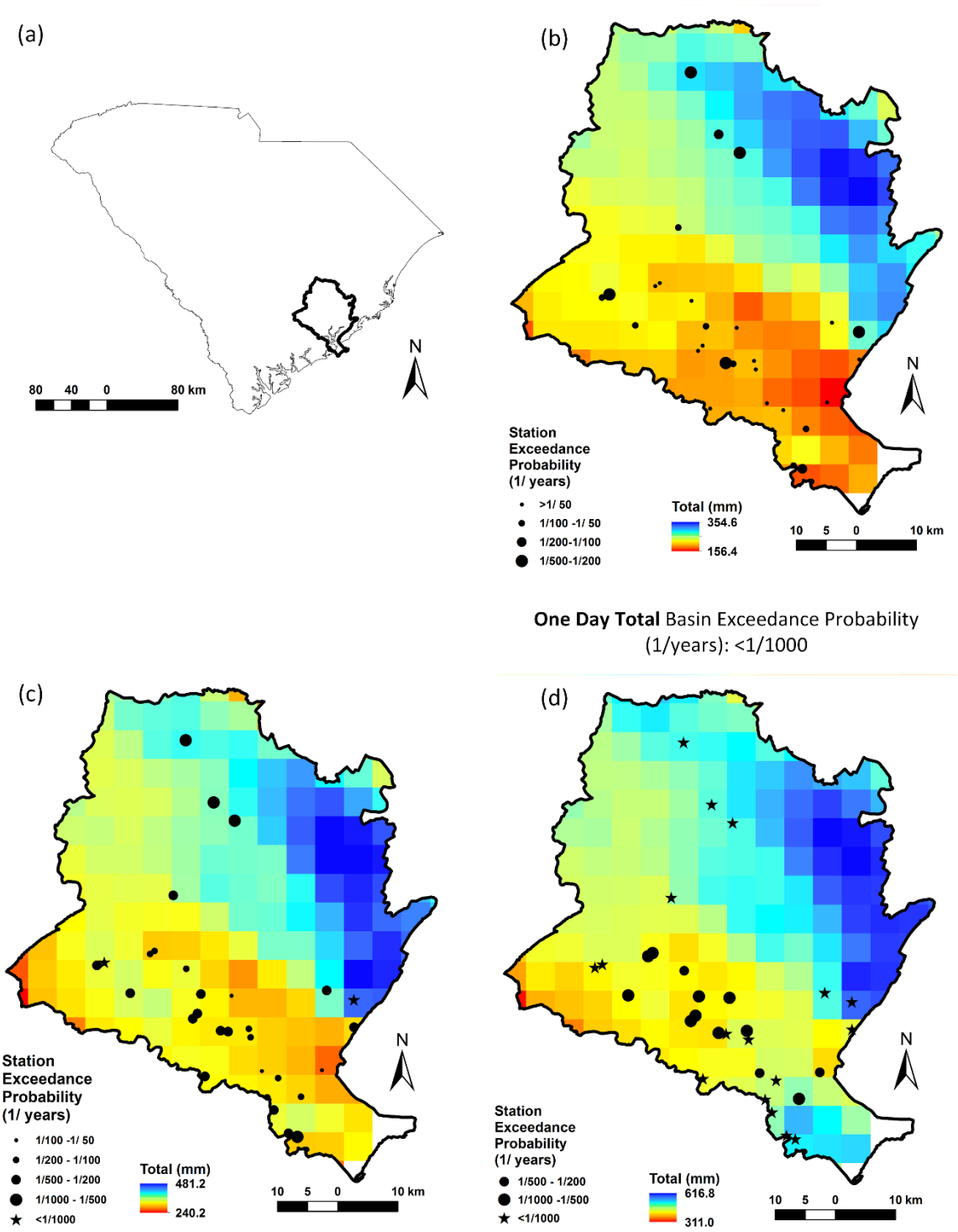
(a)
80 40 0 80 km
N
(b)
Station Exceedance Probability (1/ years)
>1/ 50
1/100 -1/ 50
1/200-1/100
1/500-1/200
Total (mm)
354.6
156.4
10 5 0 10 km
N
One Day Total Basin Exceedance Probability (1/years): <1/1000
(c)
Station Exceedance Probability (1/ years)
1/100 -1/ 50
1/200 - 1/100
1/500 - 1/200
1/1000 - 1/500
<1/1000
Total (mm)
481.2
240.2
10 5 0 10 km
N
Two Day Total Basin Exceedance Probability (1/years): < 1/1000
(d)
Station Exceedance Probability (1/ years)
1/500 - 1/200
1/1000 -1/500
<1/1000
Total (mm)
616.8
311.0
10 5 0 10 km
N
Four Day Total Basin Exceedance Probability (1/years): <1/1000

Figure 5

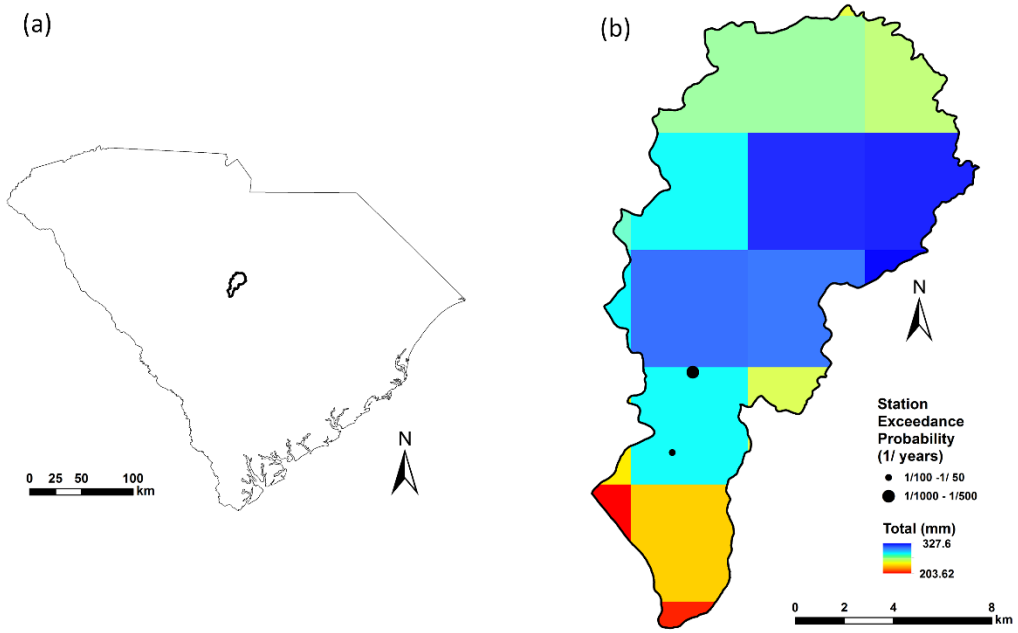

One Day Total Basin Exceedance Probability (1/years): <1/1000

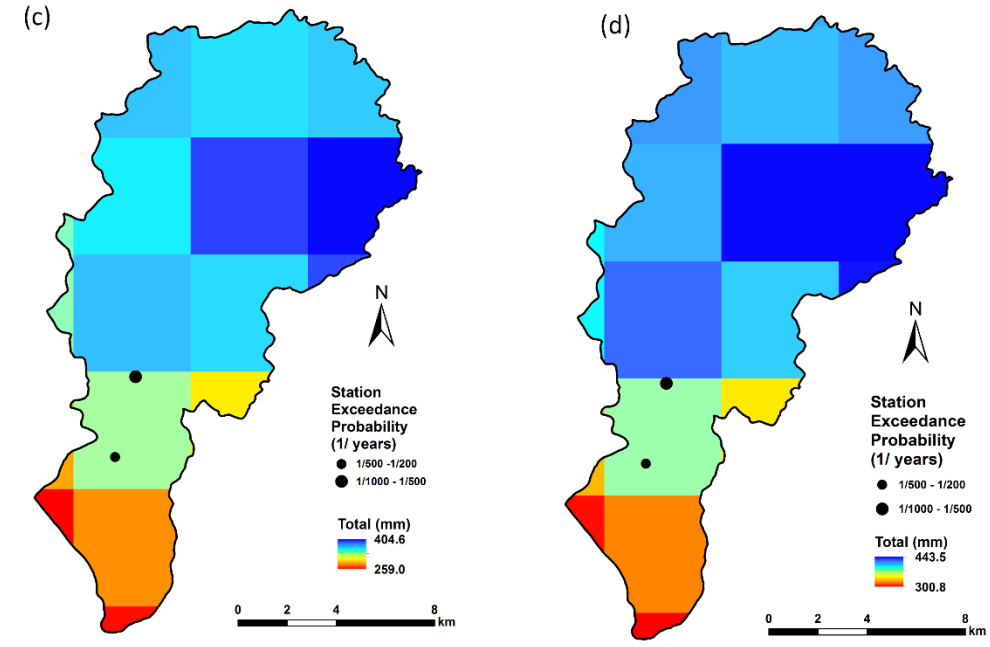

Two Day Total Basin Exceedance Probability (1/years): < 1/1000

Four Day Total Basin Exceedance Probability (1/years): <1/1000

Figure 6

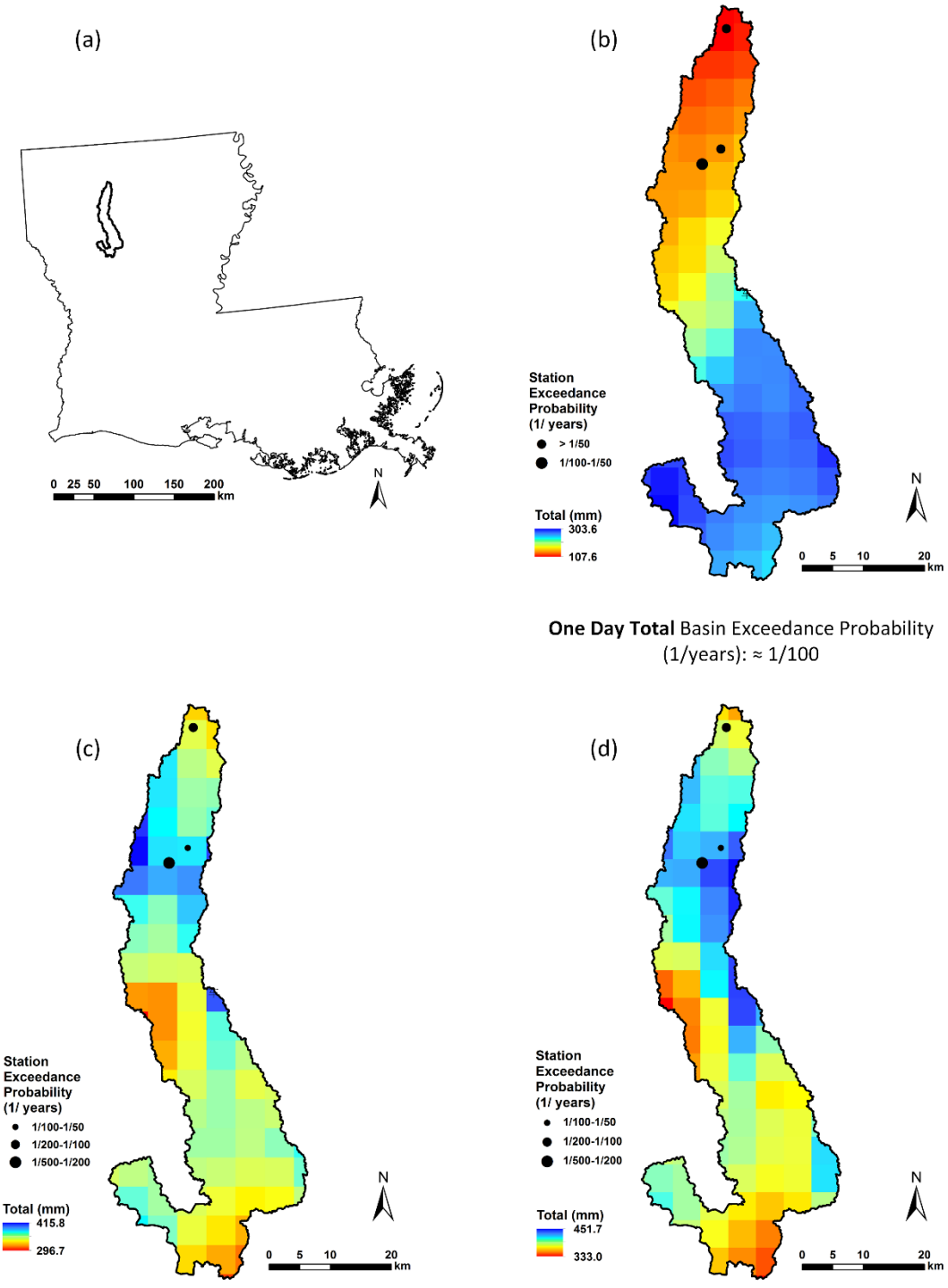

One Day Total Basin Exceedance Probability (1/years): ≈ 1/100

Two Day Total Basin Exceedance Probability (1/years): ≈ 1/400

Four Day Total Basin Exceedance Probability (1/years): 1/600-1/500

Figure 7

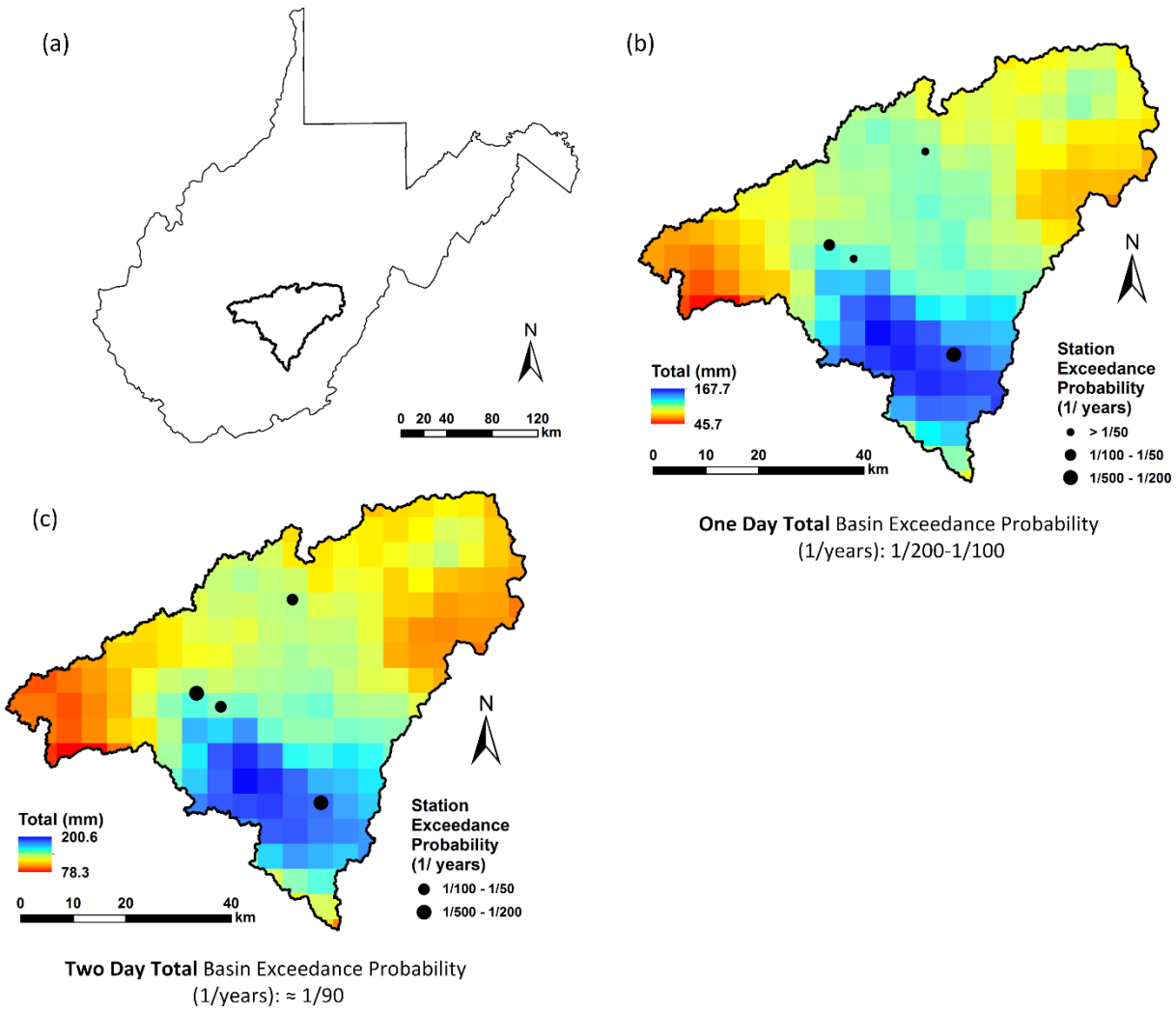
(a)
N
0 20 40 80 120
km
(b)
N
Total (mm)
167.7
45.7
0 10 20 40
km
Station
Exceedance
Probability
(1/ years)
> 1/50
1/100 - 1/50
1/500 - 1/200
One Day Total Basin Exceedance Probability
(1/years): 1/200-1/100
(c)
N
Total (mm)
200.6
78.3
0 10 20 40
km
Station
Exceedance
Probability
(1/ years)
1/100 - 1/50
1/500 - 1/200
Two Day Total Basin Exceedance Probability
(1/years): ≈ 1/90

Figure 8

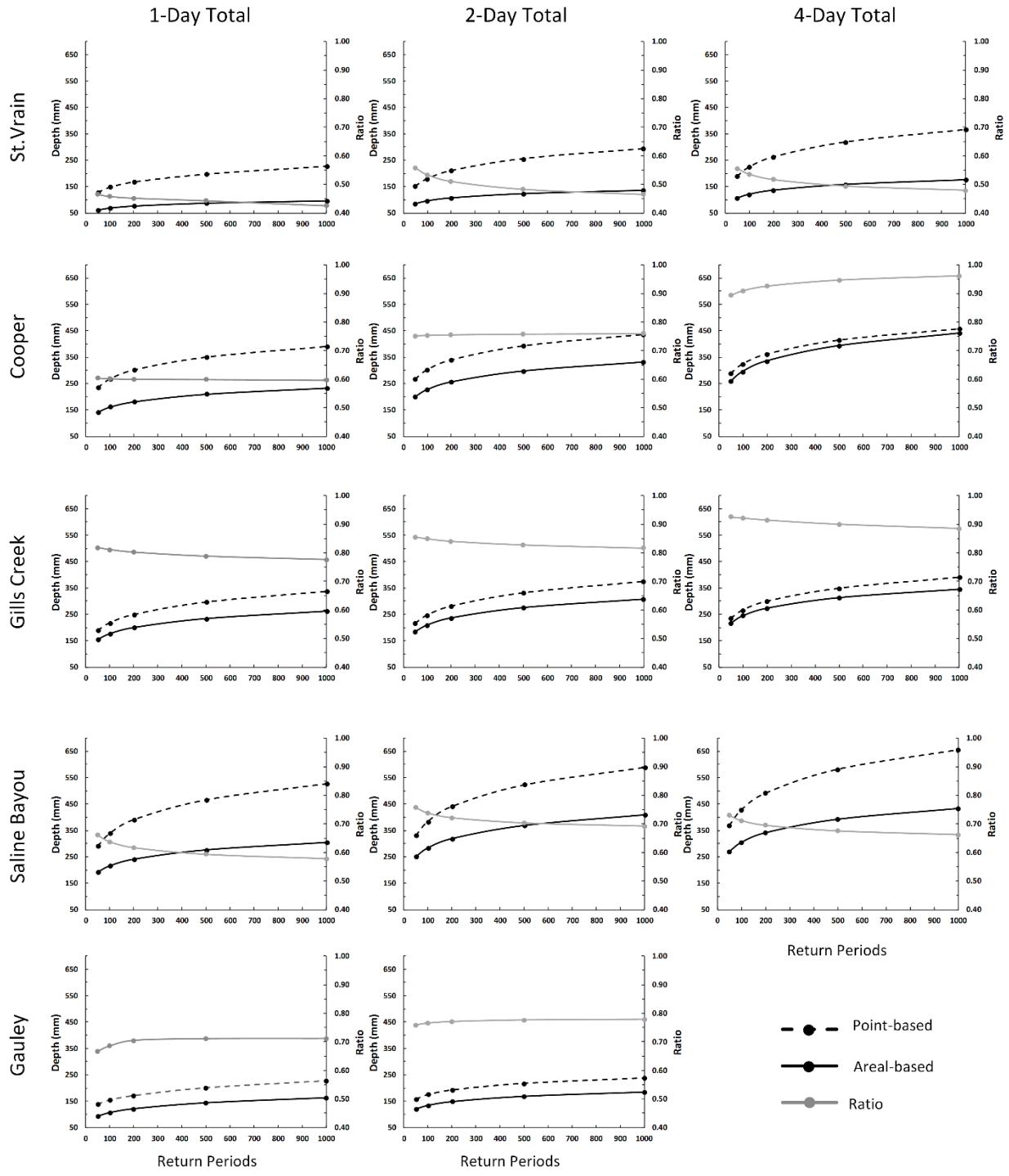

676

677 Figure 9

Table 1. Heavy rainfall events and associated watersheds.

Events		Examined Watersheds	Hydrologic Unit Code	Area	Regions for Bootstrap		
Location	Month			(km^2)	1-Day Total	2-Day Total	4-Day Total
WA, OR, and ID	Feb-1996	Wilson-Trusk-Nestuccu, OR	17100203	2951	1	1	1
CO	Sep-2013	St. Vrain, CO	10190005	2539	2	2	2
SC and NC	Oct-2015	Cooper, SC	03050201	3275	4	5	4 and 5
		Gills Creek, SC	0305011002	193	4	4	4
TX and LA	Mar-2016	Saline Bayou, LA	011140208	1266	5	6	5
WV	Jun-2016	Gauley, WV	05050005	3678	3	3	NA

Table 2 Number of stations in each exceedance probability interval based on point data (*Atlas-14*), and area-based exceedance probability.

Watershed	Duration	Exceedance Probability						
		Station/Point-based						Area-based
		> 1/50	1/100 - 1/50	1/200 - 1/100	1/500 - 1/200	1/1000 - 1/500	< 1/1000	
St. Vrain, CO	1 day	58	7	9	8	6	5	< 1 / 600
	2 days	39	9	7	8	5	25	< 1/1000
	4 days	17	17	12	11	5	31	< 1/1000
Cooper, SC	1 day	16	7	2	5			< 1/1000
	2 days		3	8	13	4	2	< 1/1000
	4 days				3	10	17	< 1/1000
Gills Creak, SC	1 day		1			1		< 1/1000
	2 days				1	1		< 1/1000
	4 days				1	1		< 1/1000
Saline Bayou, LA	1 day	2	1					≈ 1 / 100
	2 days		1	1	1			≈ 1 / 400

	4 days		1	1	1	1 / 600 - 1 / 500
Gauley, WV	1 day	2	1		1	1 / 200 - 1 / 100
	2 days		2		2	≈ 1 / 90

Table 3 Root Mean Square Error (RMSE) of bootstrapped estimated rainfall depths (mm) for each recurrence interval.

Watersheds	Durations	Recurrence Intervals							
		50	100	200	400	500	600	800	1000
Saline Bayou	1 day	3.0	4.0	5.4	7.1	7.7	8.2	9.1	9.8
	2 days	3.1	4.3	5.8	7.7	8.4	9.0	10.1	10.9
	4 days	5.0	6.7	8.8	11.4	12.3	13.0	14.3	15.4
Cooper	1 day	3.6	5.3	7.5	10.1	11.1	11.9	13.3	14.5
	2 days	4.2	6.1	8.5	11.6	12.7	13.7	15.3	16.7
	4 days	3.8	5.4	7.5	10.0	11.0	11.8	13.2	14.4
Gills Creek	1 day	2.2	3.4	4.9	6.8	7.5	8.1	9.2	10.0
	2 days	2.1	2.8	3.6	4.5	4.9	5.2	5.8	6.2
	4 days	3.0	4.5	6.3	8.6	9.4	10.1	11.2	12.2
St. Vrain	1 day	1.2	1.9	2.7	3.8	4.2	4.5	5.0	5.5
	2 days	1.5	2.3	3.3	4.6	5.1	5.5	6.2	6.8
	4 days	2.6	3.5	4.7	6.1	6.6	7.1	7.8	8.4

Wilson-Trusk-Nestuccu	1 day	2.1	2.9	3.8	4.9	5.3	5.6	6.2	6.6
	2 days	3.2	4.2	5.3	6.5	6.9	7.2	7.8	8.2
	4 days	4.0	5.3	6.9	8.6	9.2	9.7	10.5	11.1
Gauley	1 day	3.9	5.9	8.5	11.8	13.1	14.1	15.9	17.5
	2 days	2.4	3.7	5.3	7.3	8.0	8.6	9.7	10.5